

# Development of Degradable, pH-Sensitive Star Vectors for Enhancing the Cytoplasmic Delivery of Nucleic Acids

Yasemin Yuksel Durmaz, Yen-Ling Lin, and Mohamed E. H. ElSayed\*

The report describes the synthesis of degradable, pH-sensitive, membrane-destabilizing, star-shaped polymers where copolymers of hydrophobic hexyl methacrylate (HMA) and 2-(dimethylamino)ethyl methacrylate (DMAEMA) monomers are grafted from the secondary face of a beta-cyclodextrin ( $\beta$ -CD) core via acid-labile hydrazone linkages using atom transfer radical polymerization. The effect of the graft's molecular weight, HMA/DMAEMA molar ratio, and the fraction of DMAEMA converted to cationic N,N,N-trimethylaminoethyl methacrylate (TMAEMA) monomers on polymer's transfection capacity is systematically investigated. Results show that all star-shaped polymers condense anti-GAPDH silencing RNA (siRNA) into nanosized particles at  $\pm$  ratio  $\leq 4:1$ . Star polymers with shorter (25kDa) P(HMA-co-DMAEMA-co-TMAEMA) grafts are more efficient and less cytotoxic than carriers with longer (40kDa) grafts. The results show that increasing the ratio of hydrophobic HMA monomers in graft's composition higher than 50 mole% dramatically reduces polymer's aqueous solubility and abolishes their transfection capacity. Further, retention of DMAEMA monomers in graft's composition provide a buffering capacity that enhanced the endosomal escape and transfection capacity of the polymers. These systematic studies show that  $\beta$ -CD-P(HMA-co-DMAEMA-co-TMAEMA)<sub>4,8</sub> polymer with a 25 kDa average graft's molecular weight and a 50/25/25 ratio of HMA/DMAEMA/TMAEMA monomers is the most efficient carrier in delivering the siRNA cargo into the cytoplasm of epithelial cancer cells.

## 1. Introduction

Small interfering RNA (siRNA) are double stranded RNA molecules that can selectively hybridize with the target mRNA sequence in the cytoplasm and trigger its degradation by RNase H enzyme, which reduces the expression of the encoded gene.<sup>[1]</sup> Several preclinical investigations showed the potential of siRNA in inhibiting pathological gene expression, which proved effective in treatment of AIDS,<sup>[2]</sup> cardiovascular,<sup>[3]</sup> and neurodegenerative diseases.<sup>[4]</sup> However, transforming siRNA drug candidates into actual therapies with a defined dosing regimen remains

a significant challenge due to the lack of an efficient biocompatible carrier that can deliver the necessary dose selectively into the cytoplasm of the diseased cells while sparing neighboring healthy ones.<sup>[5]</sup> Cationic lipids,<sup>[6]</sup> polymers,<sup>[7]</sup> and peptides<sup>[5d]</sup> have been used to condense siRNA via electrostatic interaction forming ionic complexes that are internalized by endocytosis. However, these complexes are often trapped in the endosomal/lysosomal trafficking pathway where the loaded siRNA cargo is degraded, which diminishes their therapeutic activity.<sup>[8]</sup>

Amphiphilic pH-sensitive polymers have been used to complex siRNA forming "smart" particles that bypass the endosomal/lysosomal trafficking pathway and deliver their cargo into the cytoplasm.<sup>[9]</sup> These polymers utilize their unique ability to switch from a hydrophilic stealth-like conformation at physiologic pH to a hydrophobic membrane-destabilizing one in response to acidic endosomal pH gradients to rupture the endosomal membrane and release the entrapped RNA cargo into the cytoplasm to produce the desired effect.<sup>[10]</sup> pH-sensitive membrane-destabilizing polymers proved effective in

delivering plasmid DNA,<sup>[11]</sup> antisense oligodeoxynucleotides,<sup>[12]</sup> siRNA,<sup>[13]</sup> and proteins<sup>[14]</sup> into the cytoplasm of multiple cells both in vitro<sup>[12,13]</sup> and in vivo.<sup>[15]</sup> These amphiphilic polymers typically incorporate ionizable acidic moieties, hydrophobic motifs, and cationic groups for sensing the change in environmental pH, disruption of the endosomal membrane, and complexation of the loaded DNA/RNA, respectively.<sup>[16]</sup> Earlier research showed that the membrane-destabilizing activity increases with the increase in polymer's molecular weight.<sup>[17]</sup> However, given their non-degradable composition, these polymers are poorly eliminated by urinary excretion in vivo, which increases the risk of their long term accumulation leading to non-specific toxicity.<sup>[17b]</sup> In addition, increasing the number of hydrophobic motifs to enhance the membrane-disruptive activity dramatically reduced polymer's aqueous solubility and therapeutic utility.<sup>[17b]</sup> Further, increasing the molar fraction of the cationic group to increase DNA/RNA loading and incorporation of targeting ligands (e.g., sugars, antibody fragments) has been shown to diminish the membrane-destabilizing activity of the formed particles and reduce the associated transfection capacity.<sup>[18]</sup>

Dr. Y. Y. Durmaz, Y.-L. Lin, Prof. M. E. H. ElSayed  
University of Michigan  
Department of Biomedical Engineering  
1101 Beal Avenue  
Lurie Biomedical Engineering Building  
Ann Arbor, MI 48109, USA  
E-mail: melsayed@umich.edu



DOI: 10.1002/adfm.201203762

Polyethyleneimine (PEI) and polyamidoamine (PAMAM) dendrimers represent another class of cationic polymers that resist the drop in endosomal pH through the buffering effect of their secondary and tertiary amine groups, which causes endosomal swelling and rupture resulting in leakage of its contents into the cytoplasm.<sup>[7,19]</sup> Many targeting ligands have been covalently conjugated to PEI- and PAMAM-based complexes and proved effective in achieving selective internalization by diseased cells.<sup>[20]</sup> However, formulation of stable and efficient ionic complexes requires 10- to 20-fold N/P (+/-) ratio resulting in the use of excess polymer, which leads to significant toxicity both in vitro and in vivo.<sup>[21]</sup>

To address the limitations of both amphiphilic pH-sensitive membrane-destabilizing and endosomal buffering polymers, we report the synthesis of degradable, pH-sensitive, membrane-destabilizing, star-shaped polymers that proved efficient in delivering siRNA past the endosomal membrane and into the cytoplasm of multiple cell lines achieving the desired gene knockdown at the mRNA and protein levels. Specifically, we utilize  $\beta$ -cyclodextrin ( $\beta$ -CD), which is a Federal Drug Administration (FDA)-approved, water-soluble, cone-shaped oligosaccharide composed of seven glucose units linked by  $\alpha$ -1,4-glycosidic linkages as the core for the star-shaped vectors.<sup>[22]</sup> The  $\beta$ -CD core has seven primary hydroxyl groups at the C-6 position and fourteen secondary hydroxyl groups at the C-2 and C-3 positions providing two rims of hydroxyl groups with different chemical reactivity, which can be asymmetrically functionalized to display different motifs.<sup>[23]</sup> Therefore, we grafted amphiphilic membrane-destabilizing polymers from the secondary face of the  $\beta$ -CD core via acid-labile hydrazone linkages while leaving the primary face for subsequent modification aimed at achieving cell specific targeting (Figure 1A). We grafted a random copolymer of hydrophobic hexyl methacrylate (HMA) and pH-sensitive 2-(dimethylamino) ethyl methacrylate (DMAEMA) monomers from the secondary face of the  $\beta$ -CD core via acid-labile hydrazone linkages forming star-shaped polymer where DMAEMA monomers were partially (50%) or fully (100%) quaternized into cationic *N,N,N*-trimethylaminoethyl methacrylate iodide (TMAEMA) for complexation of siRNA molecules. We hypothesized that star-shaped  $\beta$ -CD-poly(hexyl methacrylate-*co*-(2-(dimethylamino)ethyl methacrylate)-*co*-(*N,N,N*-trimethylaminoethyl methacrylate iodide))<sub>n</sub> ( $\beta$ -CD-P(HMA-*co*-DMAEMA-*co*-TMAEMA))<sub>n</sub> polymers will condense siRNA into pH-sensitive particles that will be internalized via adsorptive-mediated

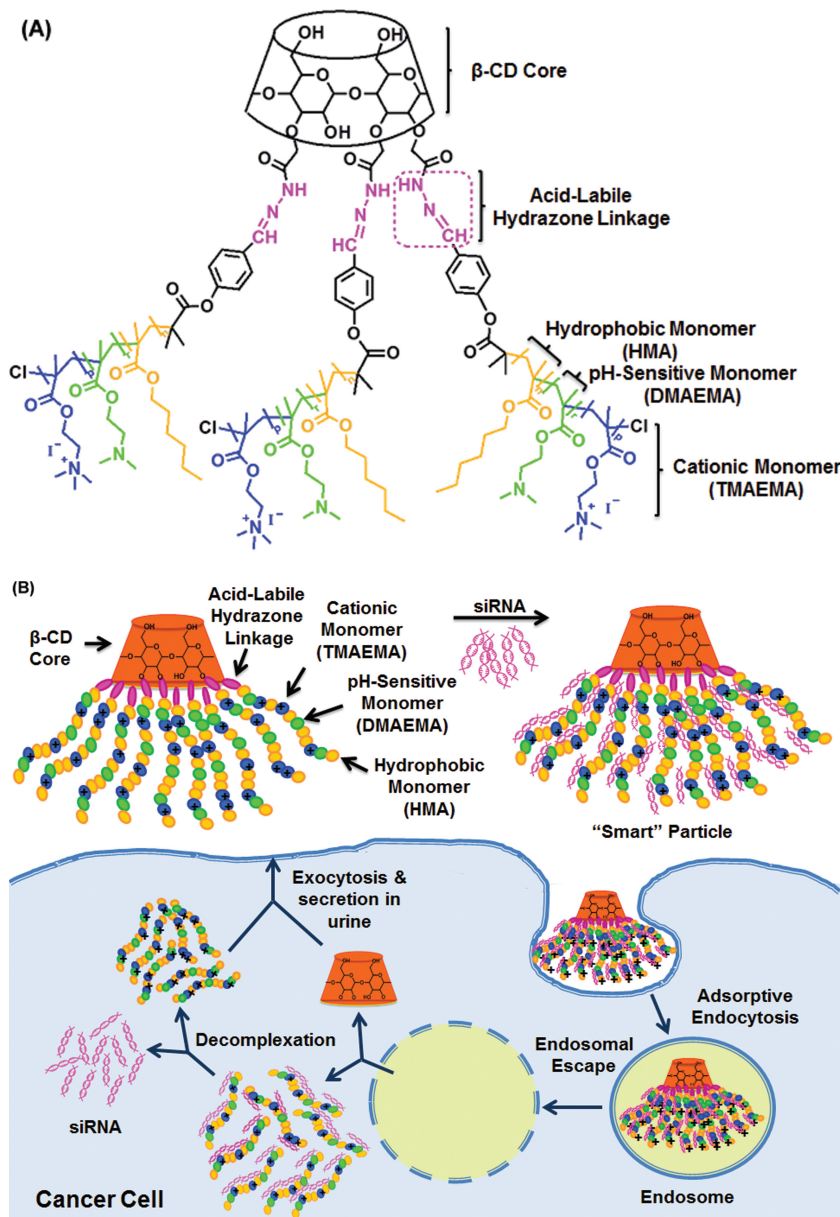


**Figure 1.** A) Structure of pH-sensitive star-shaped  $\beta$ -CD-P(HMA-*co*-DMAEMA-*co*-TMAEMA)<sub>n</sub> polymers. B) A schematic drawing showing condensation of siRNA molecules by star-shaped pH-sensitive polymers forming "smart" particles, which are internalized by endocytosis. In the endosome, acid-labile hydrazone linkages are hydrolyzed by the acidic pH and release the P(HMA-*co*-DMAEMA-*co*-TMAEMA) grafts, which rupture the endosomal membrane and release the loaded siRNA cargo into the cytoplasm.

endocytosis. In the endosome, the acid-labile hydrazone linkages will hydrolyze releasing the membrane-active poly(hexyl methacrylate-*co*-(2-(dimethylamino)ethyl methacrylate)-*co*-(*N,N,N*-trimethylaminoethyl methacrylate iodide)) (P(HMA-*co*-DMAEMA-*co*-TMAEMA)) grafts from the  $\beta$ -CD core to destabilize the endosomal membrane and release the siRNA cargo into the cytoplasm (Figure 1B).

We used atom transfer radical polymerization (ATRP) technique to control the number, molecular weight (25 and 40 kDa), and molar ratio of HMA/DMAEMA monomers

**Table 1.** Composition of the degradable, pH-sensitive, star-shaped vectors.

Polymer Code	$M_n$ of each arm <sup>a)</sup> [kDa, Kg/mol]	Copolymer composition <sup>a)</sup> [% HMA/DMAEMA]	# of HMA units <sup>a)</sup>	# of DMAEMA units <sup>a)</sup>	# of TMAEMA units <sup>a)</sup>	% of Quaternization <sup>a)</sup>
$\beta$ -CD-1	25.6	47:53	73	26	58	69
$\beta$ -CD-2	25.6	47:53	73	0	84	100
$\beta$ -CD-3	40.8	49:51	122	57	70	55
$\beta$ -CD-4	40.8	49:51	122	0	127	100
$\beta$ -CD-5	25.0	76:24	113	20	19	46
$\beta$ -CD-6	25.0	74:26	110	0	39	100
$\beta$ -CD-7	41.2	76:24	186	31	29	49
$\beta$ -CD-8	41.2	76:24	186	0	60	100

<sup>a)</sup>Calculated from the <sup>1</sup>H NMR spectra.

(50/50 and 75/25) in the grafted poly(hexyl methacrylate-*co*-(2-(dimethylamino)ethyl methacrylate)) (P(HMA-*co*-DMAEMA)) polymers to investigate the effect of the molecular weight and the hydrophobic/hydrophilic balance of these membrane-active fragments on the endosomal escape capacity indicated by the effect of the siRNA cargo. It is important to note that DMAEMA monomers have been shown to exhibit gradual protonation with the drop in environment pH producing an appreciable endosomal buffering capacity.<sup>[24]</sup> Comparing the transfection capacity of “smart” pH-sensitive particles that incorporate the same star-shaped  $\beta$ -CD carrier with identical graft composition but differ in the percentage of residual DMAEMA monomers that were not converted to cationic TMAEMA (i.e., retained their buffering capacity) allowed us to investigate the possibility of combining hydrophobic membrane disruption with endosomal burst to achieve enhanced cytoplasmic delivery and the relative contribution of each mechanism to carrier activity.

## 2. Results and Discussion

### 2.1. Synthesis of Degradable, pH-Sensitive, Star-Shaped Polymers

As described in the associated Supporting Information, we successfully utilized the asymmetric distribution of primary and secondary hydroxyl groups on opposite faces of the  $\beta$ -CD core to graft amphiphilic P(HMA-*co*-DMAEMA) polymers from the secondary face via acid-labile hydrazone linkages using ATRP. We engineered these star-shaped polymers to systematically evaluate the effect of graft's molecular weight (25 and 40 kDa), hydrophobic/hydrophilic balance defined by the ratio of HMA/DMAEMA monomers (50/50 and 75/25), and degree of quaternization of DMAEMA monomers (50% and 100%) on the complexation of siRNA molecules into “smart” particles and their ability to deliver the RNA cargo past the endosomal membrane and into the cytoplasm of epithelial cancer cells. Specifically, we controlled the molecular weight of the P(HMA-*co*-DMAEMA) grafts in  $\beta$ -CD-1, -2, -5, and -6 polymers to be  $\approx$ 25 kDa compared to  $\approx$ 40 kDa in  $\beta$ -CD-3, -4, -7, and -8 polymers (Table 1). Earlier research showed the significant

contribution of hydrophobic monomers (e.g., HMA) to the endosomal escape of ionic complexes.<sup>[17b,18a,18b]</sup> Therefore, we increased the ratio of HMA/DMAEMA monomers from 50/50 in  $\beta$ -CD-1, -2, -3, and -4 polymer to 75/25 in  $\beta$ -CD-5, -6, -7, and -8 polymers (Table 1) to examine the effect of HMA ratio on polymer's aqueous solubility and transfection efficiency of the formed complexes. Earlier research also showed that poly(2-(dimethylamino)ethyl methacrylate) (PDMAEMA) polymers exhibit higher transfection efficiency compared to poly(N,N,N-trimethylaminoethyl methacrylate) (PTMAEMA) polymers with similar molecular weight,<sup>[25]</sup> which is attributed to the endosomal buffering capacity of PDMAEMA polymers ( $pK_a = 7.5$ ) resulting in efficient destabilization of the endosomal membrane and release of the loaded nucleic acid cargo into the cytoplasm.<sup>[24]</sup> Therefore, we compared the transfection capacity of  $\beta$ -CD-1, -3, -5, and -7 polymers that have 50% of DMAEMA monomers converted to cationic TMAEMA to the transfection efficiency of  $\beta$ -CD-2, -4, -6, and -8 polymers with 100% of DMAEMA monomers converted to TMAEMA (Table 1).

The motivation to incorporate acid-labile hydrazone linkages in polymer composition is to engineer a carrier with a large number of cationic and hydrophobic groups necessary for complexation of a large dose of siRNA molecules and endosomal escape of the formed particles, which will degrade into small membrane-active fragments that can be eliminated by urinary excretion, which will address the long-term accumulation of linear non-degradable polymers and the associated in vivo toxicity.<sup>[26]</sup> Our results show that the average degradation half life ( $t_{1/2}$ ) of the acid-labile hydrazone linkages in star-shaped  $\beta$ -CD polymers incubated in an acidic buffer solution (pH 5.8) at 37 °C is 60 min  $\pm$  2 min (Figure S7, Supporting Information), which is consistent with previously published results.<sup>[13]</sup> We used the  $\beta$ -CD core to develop new star-shaped carriers for delivery of siRNA based on the established advantages of the star architecture compared to the linear counterpart.<sup>[27]</sup> For example, 3- and 5-arms star PDMAEMA polymers exhibit higher transfection efficiency and lower toxicity compared to the corresponding linear polymers with the transfection efficiency and biocompatibility increasing with the increase in degree of polymer branching.<sup>[28]</sup> This is further supported by the reported high transfection efficiency of particles prepared using dendrimers<sup>[29]</sup> and hyperbranched cationic polymers<sup>[30]</sup>

that provide steric protection for loaded cargo, long retention in the systemic circulation, and high accumulation in the tumor tissue. Therefore, distributing the number of cationic TMAEMA groups necessary for condensation of siRNA molecules over multiple polymer grafts in a star-like conformation will eliminate the significant cytotoxicity observed with the linear conformation particularly at high molecular weights.<sup>[27b,31]</sup>

ATRP<sup>[32]</sup> and reversible addition fragmentation chain transfer (RAFT)<sup>[33]</sup> polymerization techniques are the two most efficient methods to synthesize well-defined block,<sup>[34]</sup> graft,<sup>[35]</sup> and star-shaped<sup>[27b,31c,36]</sup> polymeric carriers. We utilized ATRP to control the number, molecular weight, molecular weight distribution, composition, architecture, and site-specific functionality of the formed star-shaped polymers (Table 1). It is important to note that the asymmetric grafting of P(HMA-co-DMAEMA) polymers from the secondary face of the  $\beta$ -CD core is engineered to allow selective coupling of hydrophilic poly(ethylene glycol) (PEG) chains to the primary hydroxyl groups via non-degradable linkages, which will confer resistance to the formed “smart” particles against the adsorption of serum proteins, increase their residence time in the systemic circulation, and allow passive accumulation in tumor tissue when administered in vivo. These PEG chains can be further functionalized to display an array of targeting ligands to allow cell-specific internalization and delivery of the loaded cargo.

## 2.2. Formulation of “Smart” Particles

We evaluated the ability of different star polymers ( $\beta$ -CD-1 to  $\beta$ -CD-8) to complex 0.7  $\mu$ g of anti-GAPDH (glyceraldehyde 3-phosphate dehydrogenase) siRNA at different (+/-) nitrogen (N)/phosphate (P) ratios using the standard gel retardation assay. The amount of  $\beta$ -CD polymer mixed with the anti-GAPDH siRNA was calculated based on the cationic TMAEMA content to take into account the difference in the percentage of quaternized DMAEMA monomers in each polymer composition. Results show that all  $\beta$ -CD polymers successfully condensed the loaded siRNA into particles that were retained into the loading wells at low N/P ratios (Figure 2). Comparing between  $\beta$ -CD-1 and  $\beta$ -CD-3, which have a similar number of P(HMA-co-DMAEMA-co-TMAEMA) grafts, similar HMA/DMAEMA ratio, and  $\approx$ 50% of DMAEMA monomers quaternized into TMAEMA units but differ in the molecular weight of the grafts shows that  $\beta$ -CD-3 polymer fully condenses the loaded siRNA at N/P ratio of 1.5/1 whereas full RNA condensation with  $\beta$ -CD-1 occurs at N/P ratio of 2.5/1 (Figure 2A,C). This shows that higher molecular weight of the P(HMA-co-DMAEMA-co-TMAEMA) graft (40 kDa) in  $\beta$ -CD-3 compared to  $\beta$ -CD-1 (25 kDa) results in a more efficient condensation of the loaded siRNA molecules while using a smaller (2  $\mu$ g) amount of  $\beta$ -CD-3 polymer compared to 3  $\mu$ g of  $\beta$ -CD-1. Similarly,  $\beta$ -CD-1 and  $\beta$ -CD-2 have identical number of polymeric grafts with the same molecular weight (25 kDa) and the same number of HMA and DMAEMA monomers attached to the  $\beta$ -CD core but differ in the percentage of DMAEMA monomers transformed to cationic TMAEMA complex the loaded siRNA molecules at N/P ratios of 2.5/1 and 1.5/1, respectively (Figure 2A,B). This is not surprising given that 100% of DMAEMA monomers were

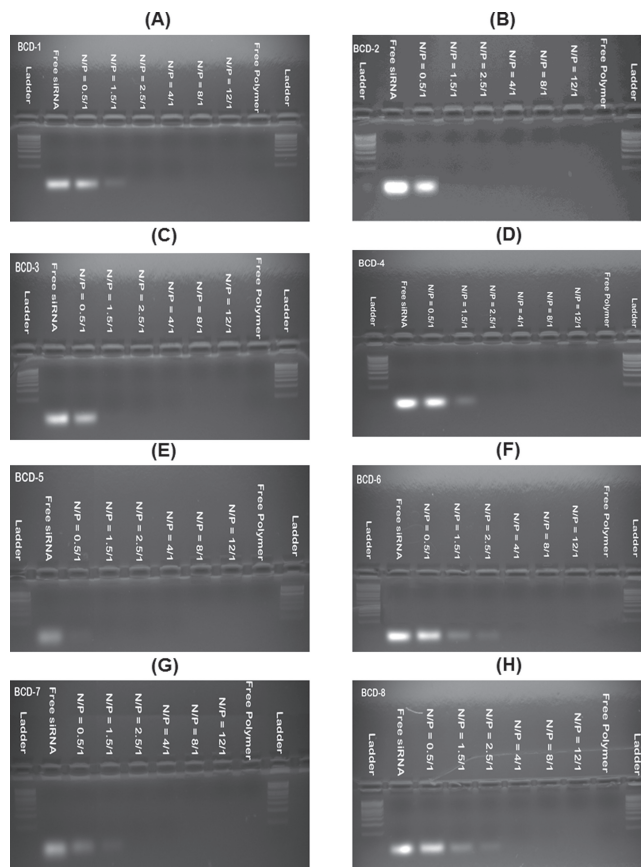


**Figure 2.** Images of the 1% w/v agarose gel containing ethidium bromide showing the electrophoretic mobility of free siRNA and the particles prepared by complexation of  $\beta$ -CD-1 to  $\beta$ -CD-8 (A-H) polymers with anti-GAPDH siRNA (0.7  $\mu$ g) at different N/P (+/-) ratios.

transformed to cationic TMAEMA in  $\beta$ -CD-2, which allows tighter binding to siRNA phosphate groups compared to partially quaternized  $\beta$ -CD-1 polymer. This led to the use of only 1  $\mu$ g of  $\beta$ -CD-2 compared to 3  $\mu$ g of  $\beta$ -CD-1 to complex the same amount of anti-GAPDH siRNA molecules.

Increasing the molar ratio of HMA/DMAEMA monomers from 50/50 (e.g.  $\beta$ -CD-2) to 75/25 (e.g.  $\beta$ -CD-6) increased the N/P ratio and amount of polymer needed to complex the loaded siRNA molecules. Specifically,  $\beta$ -CD-2 and  $\beta$ -CD-6 polymers complex equal amounts of anti-GAPDH siRNA at N/P ratios of 1.5/1 and 4/1, respectively (Figure 2B,F). This increase in the amount (6  $\mu$ g) of  $\beta$ -CD-6 polymer and the N/P ratio where full condensation of the loaded siRNA is observed as a result of the reduction in the number of cationic TMAEMA monomers/graft available for complexation with the anionic phosphate groups. Further, increasing the fraction of hydrophobic HMA monomers in graft composition reduced the aqueous solubility of the formed star polymer particularly the partially (50%) quaternized  $\beta$ -CD-5 and  $\beta$ -CD-7 polymers. It is important to note that all the synthesized  $\beta$ -CD carriers successfully complexed the loaded siRNA molecules at N/P ratios that are much lower than established transfection reagents like PEI and cationic PAMAM dendrimers, which are routinely used at N/P

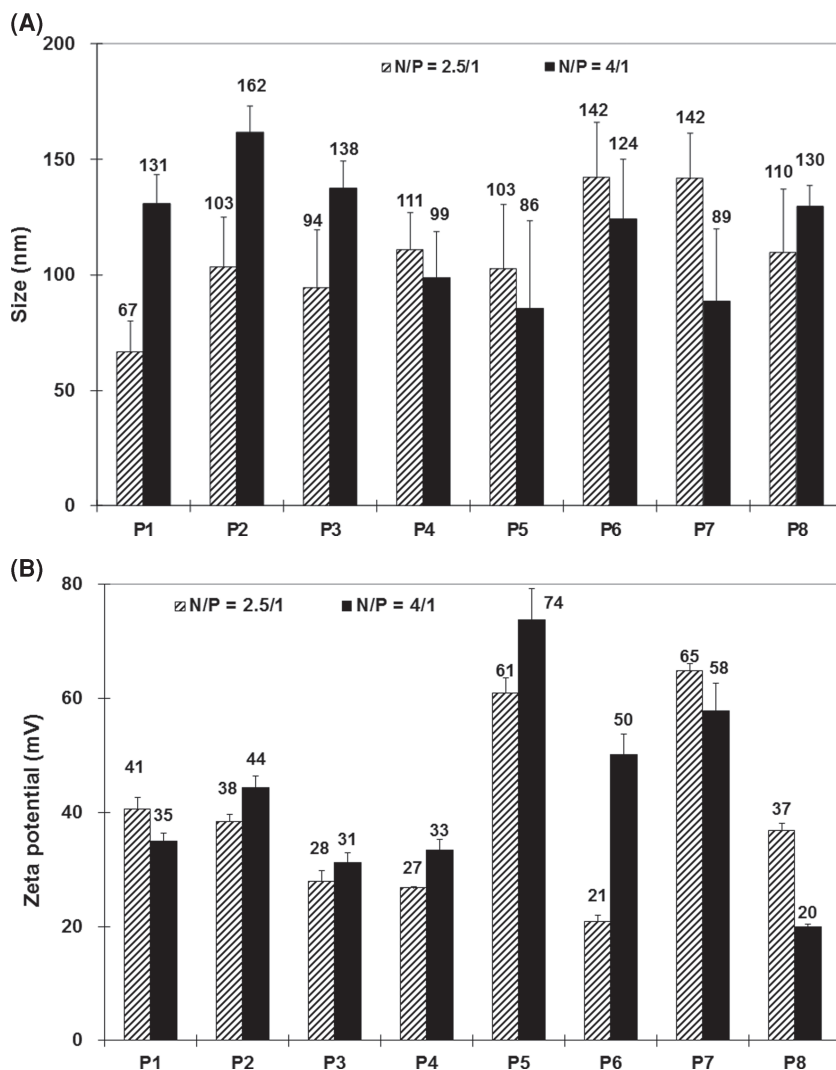


**Figure 3.** A) Size and B) surface charge of “smart” particles (P1–P8) prepared by complexation of  $\beta$ -CD-1 to  $\beta$ -CD-8 star polymers with anti-GAPDH siRNA (10.3  $\mu$ g) at N/P (+/–) ratios of 2.5/1 and 4/1. Results are the average + the standard error of the mean of two independent experiments with each experiment carried out in triplicates.

ratios  $>15/1$ .<sup>[37]</sup> This is a significant improvement over existing carriers as it allows the use of small amounts of  $\beta$ -CD-based vectors for condensation and delivery of a high dose of siRNA molecules, which will eliminate the need for excess cationic carrier and reduce the associated side effects.

### 2.3. Characterization of “Smart” Particles

All star polymers ( $\beta$ -CD-1 to  $\beta$ -CD-8) were mixed with 10.3  $\mu$ g of anti-GAPDH siRNA at N/P ratios of 2.5/1 and 4/1 to prepare “smart” particles (P1–P8) that were characterized in terms of size and surface charge using dynamic light scattering and zeta potential measurements, respectively. Results show that particle size ranged between 67–142 nm for those prepared at N/P ratio of 2.5/1, which increased to 86–162 nm for particles prepared at N/P ratio of 4/1 (Figure 3A). Given that the molecular size cut off for tumor vasculature is between 400 and

600 nm,<sup>[38]</sup> these “smart” particles (P1–P8) are suited for delivery of siRNA into solid tumors. Zeta potential measurements show that P1–P8 prepared at N/P ratio of 2.5/1 have a net positive charge of 21–65 mV, which increased to 20–74 mV for particles prepared at N/P ratio of 4/1 (Figure 3B). The cationic surface of these “smart particles (P1–P8) will trigger efficient internalization by epithelial cancer cells via adsorptive endocytosis.<sup>[13,39]</sup>

### 2.4. Uptake of “Smart” Particles into HeLa Cervical Cancer Cells

We prepared fluorescently labeled particles (P1–P8) by complexation of  $\beta$ -CD-1 to  $\beta$ -CD-8 polymers with FAM-labeled anti-GAPDH siRNA at N/P ratios of 1.5/1, 2.5/1, and 4/1 and evaluated their uptake into HeLa cervical cancer cells in comparison to free siRNA and siPORT amine-based complexes using flow cytometry. Results show that free siRNA molecules were not internalized and require a carrier to enhance their uptake by HeLa cells (Figure 4). All the particles (P1–P8) formulated at N/P ratios of 1.5/1 and 2.5/1 were internalized by  $\geq 80\%$  of HeLa cancer cells except for P7. Further, P5 and P7 particles prepared at a N/P ratio of 4/1 were poorly internalized by HeLa cells (Figure 4). The observed drop in number of fluorescently-labeled HeLa cells upon incubation with P5 and P7 particles can be attributed to higher positive surface charge density (Figure 3B), which could lead to cell death as shown with other cationic particles.<sup>[18c,18d]</sup> Consequently, we limited our study to “smart” particles (P1–P8) prepared at N/P ratio of 2.5/1 and investigated their ability to deliver anti-GAPDH siRNA into the cytoplasm of HeLa cancer cells indicated by knockdown of GAPDH expression at the mRNA and protein levels.

### 2.5. Effect of “Smart” Particles on GAPDH Expression

The ability of “smart” particles (P1–P8) to deliver functional anti-GAPDH siRNA molecules past the endosomal membrane and into the cytoplasm of HeLa cells was assayed based on their ability to selectively knockdown GAPDH gene expression at the mRNA and protein levels. We utilized the KDaAlert GAPDH assay kit to measure the changes in GAPDH protein level upon incubation with particles that encapsulate (+) the anti-GAPDH siRNA compared to those encapsulating (–) a scrambled siRNA sequence. We utilized siPORT amine-based complexes encapsulating an equal dose of (+) anti-GAPDH siRNA molecules as a positive control to determine the maximum level of knockdown that can be achieved using a robust commercial

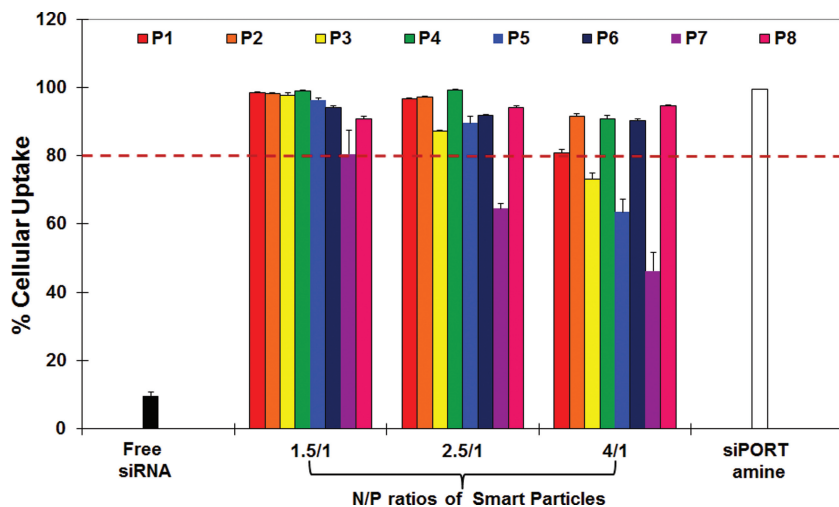


**Figure 4.** Percentage of fluorescently-labeled HeLa cancer cells after incubating for 6 h in a serum-free culture medium with free siRNA, siPORT amine-based complexes, and “smart” P1–P8 particles prepared by complexation of  $\beta$ -CD-1 to  $\beta$ -CD-8 polymers with FAM-labeled anti-GAPDH siRNA (1.14  $\mu$ g) at N/P ratios of 1.5/1, 2.5/1, and 4/1. Results are the average + the standard error of the mean of four independent experiments with each experiment carried out in triplicates.

transfection reagent (Figure 5). Results show that P1–P4 were more efficient in knocking down GAPDH protein expression compared to P5–P8 indicating that star-shaped  $\beta$ -CD carriers that incorporated equal ratios (50/50) of HMA and DMAEMA monomers were more effective in delivering the RNA cargo into HeLa cells compared to those with higher HMA content. The lack of GAPDH knockdown observed with P6 and P8 particles can be a result of poor particle solubility in culture medium whereas the non-specific GAPDH knockdown exhibited by P5 and P7 is a result of the high positive surface charge density resulting in cell death.

Results show that P1 is the most efficient formulation indicated by the  $73 \pm 1.4\%$  reduction in GAPDH protein expression observed upon incubation with P1 particles loaded with (+) anti-GAPDH siRNA compared to those loaded with (-) the scrambled siRNA sequence (Figure 5). Comparing GAPDH knockdown observed upon incubation of HeLa cells with P1 particles to that observed with P3 particles shows the effect of increasing the molecular weight of P(HMA-co-DMAEMA-co-TMAEMA) grafts from 25 kDa (P1) to 40 kDa (P3). Results show that P3 particles were partially toxic to HeLa cells indicated by the reduction in GAPDH protein expression upon treatment with (-) the scrambled siRNA sequence. Specifically, P3 particles loaded with (+) anti-GAPDH siRNA produced  $30 \pm 2.5\%$  knockdown in GAPDH expression compared to the  $73 \pm 1.4\%$  reduction observed with P1 particles. These results clearly show that  $\beta$ -CD polymers incorporating

P(HMA-co-DMAEMA-co-TMAEMA) grafts with an average molecular weight of  $\approx 25$  kDa are more efficient than longer grafts in delivery of functional siRNA into HeLa cancer cells (Figure 5). These findings are supported by recently published results showing that 3- and 5-arm branched PDMAEMA polymers exhibit measurable transfection of CHO-K1 cells at an average molecular weight  $\geq 20$  kDa.<sup>[28]</sup> However, PDMAEMA carriers with much higher molecular weight exhibited high cellular toxicity that diminished their transfection efficiency.<sup>[28]</sup>

Comparing between GAPDH knockdown observed upon incubation of HeLa cells with P1 and P2 particles shows the contribution of the buffering capacity of DMAEMA monomers to the endosomal escape and transfection efficiency of P1 particles. Specifically, P1 particles are formulated using  $\beta$ -CD-1 polymer with 69% of the DMAEMA monomers converted to cationic TMAEMA, which leaves 31% of the DMAEMA monomers ( $pK_a = 7.5$ ) to exhibit their buffering capacity at acidic endosomal pH. Whereas, P2 particles are formulated using  $\beta$ -CD-2 polymer with 100% of DMAEMA monomers transformed to cationic TMAEMA (i.e., no endosomal buffering capacity). Results show that P2 particles loaded with (+) anti-GAPDH siRNA produce  $58 \pm 2.3\%$  knockdown in

capacity at acidic endosomal pH. Whereas, P2 particles are formulated using  $\beta$ -CD-2 polymer with 100% of DMAEMA monomers transformed to cationic TMAEMA (i.e., no endosomal buffering capacity). Results show that P2 particles loaded with (+) anti-GAPDH siRNA produce  $58 \pm 2.3\%$  knockdown in

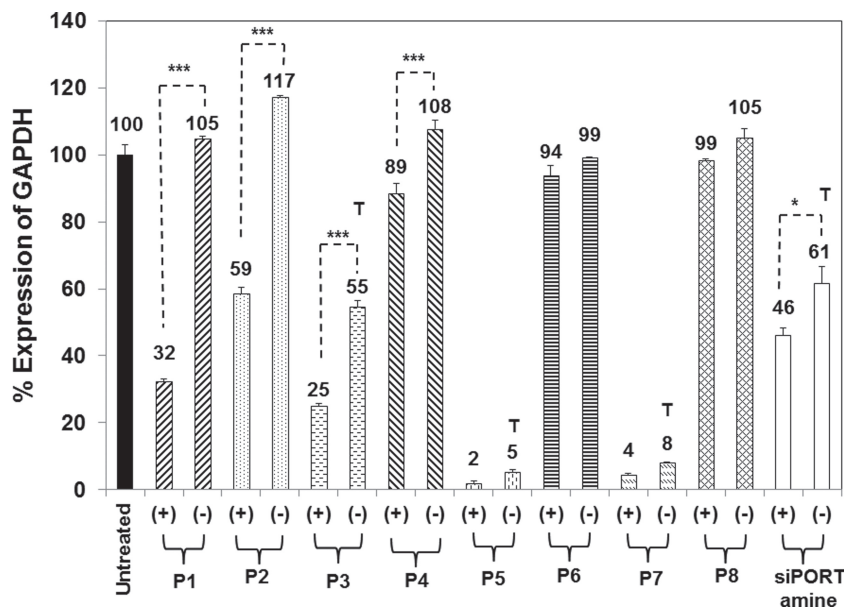


**Figure 5.** Effect of “smart” particles (P1–P8) and siPORT amine-based complexes encapsulating 200 nM of (+) anti-GAPDH siRNA or (-) a scrambled siRNA sequence on GAPDH protein expression in HeLa cervical cancer cells. P1–P8 particles were prepared by complexation of  $\beta$ -CD-1 to  $\beta$ -CD-8 with 1.14  $\mu$ g of the selected siRNA sequence at a N/P ratio of 2.5/1. Results are the average + the standard error of the mean of four independent experiments with each experiment carried out in five replicates. Statistical difference between particles encapsulating (+) anti-GAPDH siRNA and (-) scrambled siRNA sequence was evaluated using paired *t* test where \* denotes  $p \leq 0.05$ , \*\*\* denotes  $p \leq 0.005$ . T denotes non-specific GAPDH knockdown due to particle toxicity.

GAPDH protein expression compared to  $73 \pm 1.4\%$  GAPDH knockdown observed with P1 particles (Figure 5). Similarly, P4 particles (100% of DMAEMA monomers transformed to cationic TMAEMA) loaded with anti-GAPDH siRNA caused  $19 \pm 5.6\%$  reduction in GAPDH expression compared to  $30 \pm 2.5\%$  observed with P3 particles (only 55% of DMAEMA monomers transformed to cationic TMAEMA leaving 45% of DMAEMA monomers with endosomal buffering capacity) (Figure 5). Given that P1, P2, P3, and P4 particles exhibit similar uptake by HeLa cancer cells (Figure 4), higher GAPDH knockdown observed with P1 and P3 particles compared to P2 and P4 particles can be attributed to the endosomal buffering capacity of DMAEMA monomers, which results in endosomal burst and enhanced release of the loaded siRNA into the cytoplasm. These results are supported by earlier reports showing the enhanced endosomal escape of PDMAEMA through their endosomal buffering capacity.<sup>[24]</sup> It is important to note that siPORT amine-based complexes produced only  $15 \pm 7.2\%$  reduction in GAPDH protein expression and it was associated with significant toxicity indicated by GAPDH knockdown upon incubation with siPORT amine-based complexes loaded with the scrambled siRNA sequence (Figure 5).

## 2.6. Contribution of DMAEMA Monomers to Carrier's Transfection Capacity

The amount of cationic quaternary amine groups (TMAEMA) needed to complex  $1.14 \mu\text{g}$  of anti-GAPDH siRNA at N/P ratio of 2.5/1 is  $4.62 \times 10^{-8}$  moles. We used the number of TMAEMA monomers present in each  $\beta$ -CD polymer to calculate the amount of polymer needed to complex the same dose ( $1.14 \mu\text{g}$ ) of anti-GAPDH siRNA at N/P ratio of 2.5/1. Given that  $\beta$ -CD-1 polymer has only 58 TMAEMA units/graft compared to 84 TMAEMA units/graft in  $\beta$ -CD-2 polymer (Table 1), we used a higher amount of  $\beta$ -CD-1 ( $27 \mu\text{g}$ ) than  $\beta$ -CD-2 ( $21 \mu\text{g}$ ) to complex the same amount ( $1.14 \mu\text{g}$ ) of anti-GAPDH siRNA at N/P ratio of 2.5/1. We investigated whether the observed higher activity of P1 particles in reducing GAPDH protein expression compared to P2 particles is a result of the higher amount of  $\beta$ -CD-1 polymer used to complex the anti-GAPDH siRNA or the higher number of DMAEMA monomers/graft, which enhances the endosomal escape of the formed particles through their established endosomal buffering capacity. Specifically, we mixed  $27 \mu\text{g}$  of  $\beta$ -CD-1 and  $21 \mu\text{g}$  of  $\beta$ -CD-2 polymers with  $1.14 \mu\text{g}$  of (+) anti-GAPDH siRNA or (-) the scrambled sequence to prepare P1-TMAEMA and P2-TMAEMA particles at N/P ratio of 2.5/1 based on the number of cationic TMAEMA monomers present in each carrier. We also mixed  $21 \mu\text{g}$  of  $\beta$ -CD-1 polymer with  $1.14 \mu\text{g}$  of (+) anti-GAPDH siRNA or (-) the scrambled sequence to prepare P1-DMAEMA particles based on the number of DMAEMA monomers present in the  $\beta$ -CD-1 carrier. We evaluated the effect of P1-DMAEMA, P1-TMAEMA, and P2-TMAEMA particles on GAPDH expression in HeLa cervical cancer cells compared to commercial siPORT amine complexes (Figure 6).

Results show that P1-TMAEMA and P1-DMAEMA particles produce a similar knockdown in GAPDH protein expression by  $57 \pm 4.6\%$  and  $51 \pm 4.7\%$ , respectively (Figure 6A). Similarly,

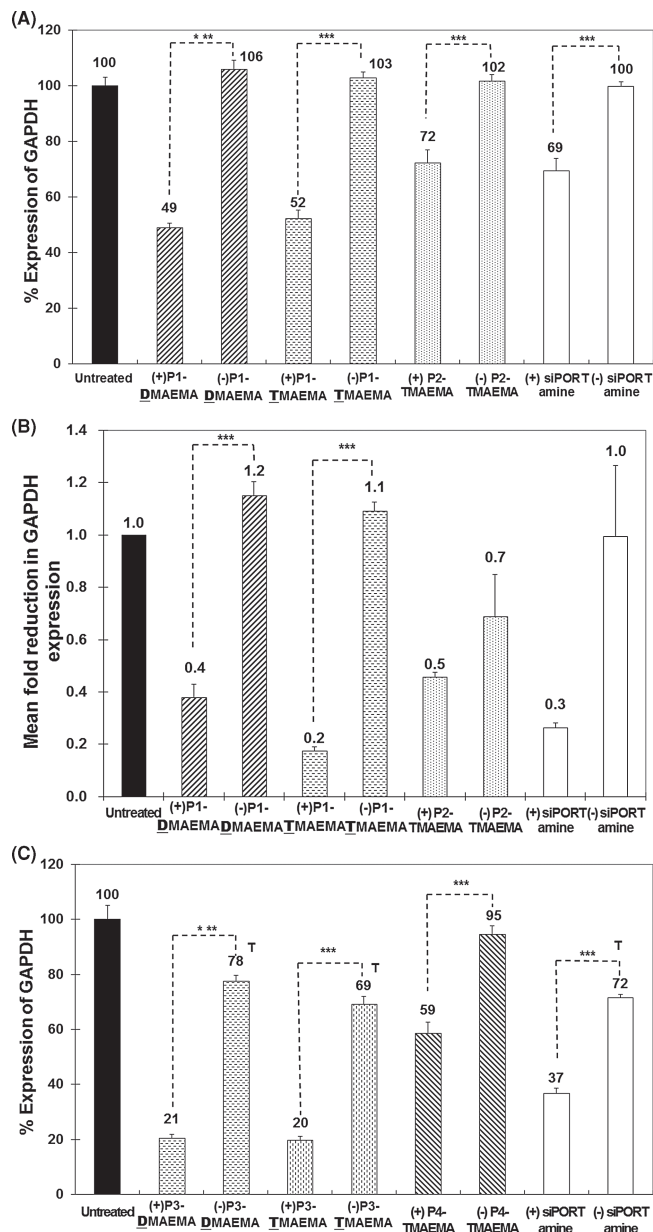


**Figure 6.** Effect of P1-DMAEMA, P1-TMAEMA, and P2-TMAEMA particles loaded with  $1.14 \mu\text{g}$  of (+) anti-GAPDH siRNA or (-) a scrambled siRNA sequence on A) GAPDH protein and B) mRNA levels in HeLa cervical cancer cells. The mRNA levels for the GAPDH gene were normalized to mRNA levels of the  $\beta$ -actin gene. C) Effect of P3-DMAEMA, P3-TMAEMA, and P4-TMAEMA particles loaded with  $1.14 \mu\text{g}$  of (+) anti-GAPDH siRNA or (-) a scrambled siRNA sequence on GAPDH protein level in HeLa cervical cancer cells. Results are the average + standard error of the mean of five replicates. Statistical difference between particles encapsulating (+) anti-GAPDH siRNA and (-) scrambled siRNA sequence was evaluated using paired *t* test where \*\*\* denotes  $p \leq 0.005$ . T denotes non-specific GAPDH knockdown due to particle toxicity.

P1-TMAEMA and P1-DMAEMA particles reduced the levels of GAPDH mRNA by  $80 \pm 10.0\%$  and  $90 \pm 5.0\%$ , respectively (Figure 6B). The fact that P1-TMAEMA particles with higher

carrier content (27  $\mu\text{g}$  of  $\beta\text{-CD-1}$ ) did not show higher activity compared to P1- $\underline{\text{DMAEMA}}$  particles (21  $\mu\text{g}$  of  $\beta\text{-CD-1}$ ) indicates that the amount of  $\beta\text{-CD-1}$  polymer does not play a significant role in the observed activity of P1 particles. In comparison, P2- $\underline{\text{TMAEMA}}$  particles reduced the levels of GAPDH protein and mRNA by only  $30 \pm 7.0\%$  and  $23 \pm 17.7\%$ , respectively (Figure 6A,B). Therefore, the observed low GAPDH knockdown by P2- $\underline{\text{TMAEMA}}$  particles compared to P1- $\underline{\text{DMAEMA}}$  and P1- $\underline{\text{TMAEMA}}$  particles is due to the residual DMAEMA monomers (26 monomers/graft) present in the  $\beta\text{-CD-1}$  carrier that exhibit an appreciable endosomal buffering capacity<sup>[24]</sup> leading to endosomal swelling and burst, which further enhances the cytoplasmic delivery of the loaded anti-GAPDH siRNA molecules.

We confirmed the contribution of DMAEMA monomers to the enhanced endosomal escape of P3 particles by comparing GAPDH knockdown by P3- $\underline{\text{DMAEMA}}$  and P3- $\underline{\text{TMAEMA}}$  particles to GAPDH knockdown observed with P4- $\underline{\text{TMAEMA}}$  particles (Figure 6C). Results show that P3- $\underline{\text{DMAEMA}}$  and P3- $\underline{\text{TMAEMA}}$  particles caused a similar knockdown of GAPDH protein expression by  $49 \pm 4.3\%$  and  $57 \pm 3.2\%$ , respectively, which further confirms that the amount of  $\beta\text{-CD-3}$  polymer used to prepare different particles at N/P ratio of 2.5/1 does not contribute to the observed activity. In comparison, P4- $\underline{\text{TMAEMA}}$  particles reduced GAPDH protein expression by  $36 \pm 6.7\%$ , which is less than the observed knockdown with both P3- $\underline{\text{DMAEMA}}$  and P3- $\underline{\text{TMAEMA}}$  particles. These results collectively show that  $\beta\text{-CD-1}$  and  $\beta\text{-CD-3}$  polymers with partially quaternized (50%) DMAEMA monomers exhibit more efficient cytoplasmic delivery of the complexed siRNA molecules compared to their fully quaternized counterparts ( $\beta\text{-CD-2}$  and  $\beta\text{-CD-4}$  polymers), which is a result of the synergistic combination of DMAEMA endosomal buffering capacity with HMA membrane-destabilizing effect on the same membrane-active P(HMA-co-DMAEMA-co-TMAEMA) grafts.

## 2.7. Cellular Uptake and Activity of P1/P2 Particles in MCF-10A and UM-SCC-17B Cells

Results show that P1 and P2 particles prepared by complexation of  $\beta\text{-CD-1}$  and  $\beta\text{-CD-2}$  polymers with anti-GAPDH siRNA at N/P ratio of 2.5/1 are efficiently internalized by HeLa cervical cancer cells (Figure 4) and achieve robust knockdown of GAPDH expression at the mRNA and protein levels (Figure 6). We investigated the uptake of P1 and P2 particles loaded with anti-GAPDH siRNA into normal human mammary epithelial cells (MCF-10A) and head and neck squamous cell carcinoma (UM-SCC-17B) and the associated knockdown in GAPDH expression to confirm the utility of these “smart” particles in multiple cell lines. Results show that “smart” P1 and P2 particles are internalized by 98–100% of MCF-10A cells at N/P ratios of 1.5/1 and 2.5/1, which drops to 76–83% of the cells upon incubation with the particles prepared at higher 4/1 N/P ratio (Figure 7A). In comparison, 93–100% of UM-SCC-17B cells internalized P1 and P2 particles prepared at N/P ratios of 1.5/1, 2.5/1, and 4/1 (Figure 7B).

We investigated the effect of “smart” P1 and P2 particles prepared by complexation of  $\beta\text{-CD-1}$  and  $\beta\text{-CD-2}$  polymers with (+)

anti-GAPDH siRNA and (-) scrambled siRNA sequence at N/P ratio of 2.5/1 using the same polymer amounts listed in section 2.5 on GAPDH expression in MCF-10A and UM-SCC-17B cells. In MCF-10A cell, P1 and P2 particles reduced GAPDH protein levels by  $31 \pm 4.6\%$  and  $25 \pm 11.2\%$ , respectively (Figure 7C). P1 and P2 particles loaded with anti-GAPDH siRNA reduced GAPDH mRNA levels by  $50 \pm 18\%$ , and  $50 \pm 38\%$ , respectively (Figure 7E). In UM-SCC-17B cancer cells, P1 and P2 particles loaded with anti-GAPDH siRNA caused a similar reduction in GAPDH protein expression by  $21 \pm 4.3\%$  and  $30 \pm 6.9\%$ , respectively (Figure 7D). However, qRT-PCR results show that only P1 particles reduced GAPDH mRNA levels by  $40 \pm 14\%$  while P2 particles did not affect GAPDH mRNA level (Figure 7F).

The observed difference in GAPDH knockdown induced by P1 and P2 particles loaded with anti-GAPDH siRNA in HeLa, MCF-10, and UM-SCC-17B cells can be explained by the difference in intracellular pH between these cells lines. The literature shows that normal cells generally have neutral cytosolic (pH 7.2) and acidic endosomal (pH 6.0) and lysosomal (pH 5.0) environment.<sup>[40]</sup> Whereas, many tumor cells have an acidified cytosol and more alkaline endosomes/lysosomes with both pH values is around 6.7.<sup>[40]</sup> Although the reason for alkalization of the endosomal and lysosomal compartments remains elusive, the elevated organelle pH in tumor cells has been confirmed in many reports<sup>[40b,41]</sup> and proved to dramatically reduce the transfection efficiency of non-viral vectors in tumor cells.<sup>[42]</sup> Similarly, low GAPDH knockdown in UM-SCC-17B cancer cells can be attributed to endosomal alkalization, which will reduce the hydrolysis of the hydrazone linkages connecting the membrane-active P(HMA-co-DMAEMA-co-TMAEMA) grafts to the  $\beta\text{-CD}$  core. Incomplete release of P(HMA-co-DMAEMA-co-TMAEMA) grafts will reduce the net disruption of the endosomal membrane, which will limit the delivery of the loaded anti-GAPDH siRNA into the cytoplasm and diminish the associated GAPDH knockdown. This explains lower GAPDH knockdown observed with P1 ( $21 \pm 4.3\%$ ) in UM-SCC-17B cancer cells compared to that observed ( $31 \pm 4.6\%$ ) with normal MCF-10A mammary epithelial cells. These results show that type of targeted cells can influence the transfection efficiency of “smart” star-shaped  $\beta\text{-CD}$  carriers. Nevertheless, our results collectively show the ability of  $\beta\text{-CD-1}$  polymers to complex siRNA at low N/P ratio and achieve efficient functional delivery of the loaded cargo into the cytoplasm of different cells.

## 3. Conclusions

In summary, we used FDA-approved, water-soluble, cone-shaped  $\beta\text{-CD}$  to prepare a series ( $\beta\text{-CD-1}$  to  $\beta\text{-CD-8}$ ) of degradable, pH-sensitive, star-shaped polymers and evaluated their ability to deliver anti-GAPDH siRNA past the endosomal membrane and into the cytoplasm of multiple epithelial cell lines. Using ATRP, we grafted P(HMA-co-DMAEMA) copolymers from the secondary face of the  $\beta\text{-CD}$  core via acid-labile hydrazone linkages. We varied the molecular weight (25 and 40 kDa), molar ratio of HMA/DMAEMA monomers (50/50 and 75/25), and degree of quaternization (50% and 100%) of DMAEMA monomers into cationic TMAEMA to systematically investigate the effect of these parameters on siRNA

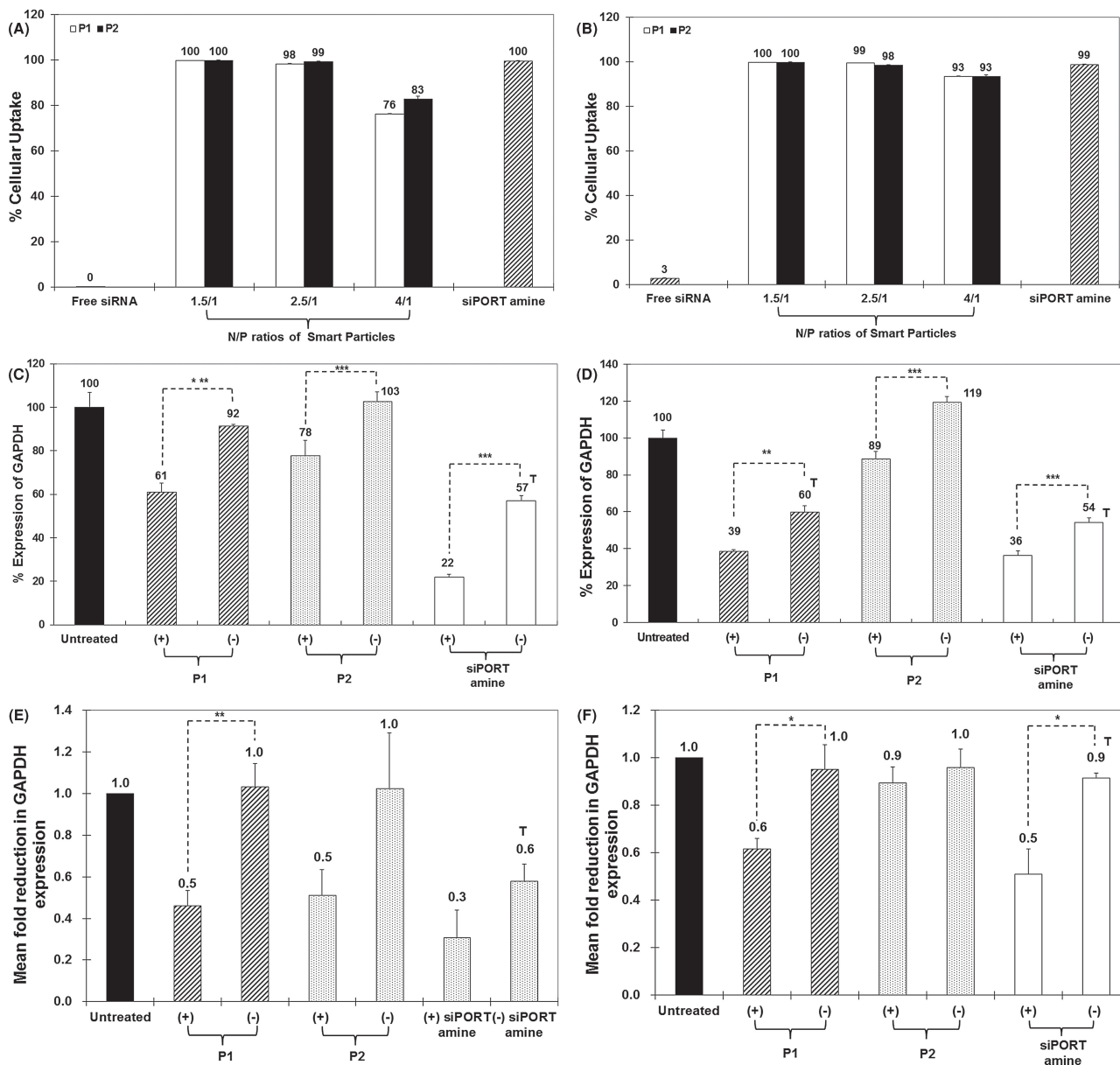


**Figure 7.** Percentage of fluorescently labeled A) MCF-10A and B) UM-SCC-17B cells that internalize free FAM-labeled anti-GAPDH siRNA molecules, “smart” P1-P2 particles encapsulating FAM-labeled anti-GAPDH siRNA, and siPORT amine-based complexes upon incubation for 6 h in a serum-free culture medium. Effect of P1 and P2 particles loaded with 1.14  $\mu\text{g}$  of (+) anti-GAPDH siRNA or (-) a scrambled siRNA sequence on GAPDH protein (C,D) and mRNA (E,F) levels in MCF-10A (C,E) and UM-SCC-17B (D,F) cells. The mRNA levels for the GAPDH gene were normalized to mRNA levels of the  $\beta$ -actin gene. Results are the average + the standard error of the mean of five replicates. Statistical difference between particles encapsulating (+) anti-GAPDH siRNA and (-) scrambled siRNA sequence was evaluated using paired *t* test where \* denotes  $p \leq 0.05$ , \*\* denotes  $p \leq 0.01$ , and \*\*\* denotes  $p \leq 0.005$ . T denotes non-specific GAPDH knockdown due to particle toxicity.

condensation into “smart” particles and the associated transfection efficiency. Results show that  $\beta$ -CD polymers incorporating 50% DMAEMA monomers/graft complex the loaded siRNA at low N/P (+/-) ratios of 1.5/1 and 2.5/1 whereas the  $\beta$ -CD polymers with lower DMAEMA content form their complexes at a 4/1 N/P ratio. The average sizes of “smart” P1-P8 particles was < 200 nm and have a net positive surface charge, which suggest their ability to diffuse from the systemic circulation into tumor’s interstitial space followed by efficient cell uptake via endocytosis

when administered in vivo. Results show that  $\beta$ -CD polymers with 25 kDa P(HMA-co-DMAEMA) grafts are more efficient in delivering the siRNA cargo compared to those with longer (40 kDa) grafts while exhibiting no cytotoxicity. Increasing the mole fraction of hydrophobic HMA monomers to 75% of the graft reduced aqueous solubility and transfection efficiency of the  $\beta$ -CD carriers compared to those with lower HMA content (50%/graft). Transforming 100% of DMAEMA monomers to cationic TMAEMA enhanced the condensation of the loading

siRNA molecules. However, combining the endosomal buffering capacity of DMAEMA monomers with the hydrophobic disruptive effect of HMA units in a single membrane-active P(HMA-co-DMAEMA-co-TMAEMA) graft proved to increase the efficiency of “smart” P1 and P3 particles by enhancing their endosomal escape. These results provide a clear description of key structural features necessary for development of efficient  $\beta$ -CD star-shaped carriers for siRNA delivery. Further, it establishes  $\beta$ -CD-1 polymer as a robust vector for enhanced cytoplasmic delivery of siRNA.

## 4. Experimental Section

**Synthesis and Characterization of Degradable, pH-Sensitive, Star-Shaped Polymers:** A series of degradable, pH-sensitive, star-shaped  $\beta$ -CD-P(HMA-co-DMAEMA-co-TMAEMA)<sub>4,8</sub> polymers were synthesized with varied molecular weight (25 or 40 kDa) of the P(HMA-co-DMAEMA-co-TMAEMA) grafts, molar ratio of HMA/DMAEMA monomers (50/50 or 75/25), and degree of quaternization (50% or 100%) of DMAEMA monomers to cationic TMAEMA to systematically investigate the effect of these parameters on their ability to deliver siRNA molecules into the cytoplasm of epithelial cells. Detailed description of the experimental procedures for the synthesis and characterization of these polymers along with the supporting spectra are provided in the Supporting Information.

**Formulation and Characterization of “Smart” Particles:** All star-shaped pH-sensitive polymers were dissolved in RNase-free water except ( $\beta$ -CD-5 and  $\beta$ -CD-7 polymers, which were dissolved in 100% DMSO before mixing with 0.7  $\mu$ g of anti-GAPDH siRNA at different N/P ratios. Each mixture was vortexed and allowed to stand at room temperature for 20 min before loading onto a 1% w/v agarose gel containing ethidium bromide (EtBr). The gel was immersed in a Tris-acetate-EDTA (TAE) buffer and run at 60 V for 45 min before visualizing under UV using a fluorescent green filter (Fotodyne Incorporated, Hartland, WI). Size and zeta potential of the particles prepared at N/P ratios of 2.5/1 and 4/1 using  $\beta$ -CD 1-8 star polymers were measured by 90Plus particle size analyzer with ZetaPALS capability (Brookhaven Instruments Corporation, Holtsville, NY).

**Cell Culture:** UM-SCC-17B head and neck squamous cell carcinoma and HeLa cervical cancer cells were generously provided by Dr. Jacques Nör (University of Michigan, School of Dentistry) and cultured following established protocols.<sup>[43]</sup> Briefly, HeLa and UM-SCC-17B cells were maintained in DMEM (Life Technologies, Grand Island, NY) supplemented with 10% fetal bovine serum (Life Technologies, Grand Island, NY), penicillin (10 000 U mL<sup>-1</sup>), and streptomycin (10 000  $\mu$ g mL<sup>-1</sup>) while regularly changing the growth medium every 2 days. MCF-10A mammary epithelial cells were generously provided by Dr. Sofia Merajver (University of Michigan, Department of Internal Medicine) and cultured in DMEM/F-12 (1:1) medium supplemented with 5% horse serum, EGF, cholera toxin, bovine insulin, and hydrocortisone. HeLa, UM-SCC-17B, and MCF-10A cells were incubated at 37 °C, 5% CO<sub>2</sub>, 95% relative humidity, and passaged upon reaching 70–90% confluency using 0.25% trypsin/EDTA mixture.

**Cellular Uptake of “Smart” Particles:** Star-shaped polymers and commercial siPORT-NH<sub>2</sub> were dissolved in OPTI-MEM solution (Life Technologies, Grand Island, NY) before mixing with 1.14  $\mu$ g of FAM-labeled anti-GAPDH siRNA (Ambion Inc, Austin, TX) at N/P ratios of 1.5/1, 2.5/1, and 4/1 to prepare different complexes, which were incubated 6 h at 37 °C, 5% CO<sub>2</sub>, and 95% relative humidity with HeLa, UM-SCC-17B, or MCF-10A cells seeded at a seeding density of  $4 \times 10^4$  cells per well. Cells were then washed with PBS, treated with 0.25% trypsin/EDTA solution for 10 min, harvested, and centrifuged to form a cell pellet and remove the supernatant medium with free particles. Cell pellets were suspended in PBS and analyzed using Biosciences FACSCalibur Flow Cytometer (Becton Dickinson, Franklin Lakes, NJ)

to determine the percentage of fluorescently-labeled cells for each treatment. Cells were gated by forward/size scatter and 10,000 gated events were collected per sample to discriminate between live and dead cells and account for live cells only.

**In Vitro Evaluation of “Smart” Particles:** HeLa, UM-SCC-17B, and MCF-10A cells were plated in 24-well plates at a seeding density of  $2 \times 10^4$  cells per well and allowed to adhere for 18 h. Different “smart” particles and siPORT-NH<sub>2</sub> complexes incorporating anti-GAPDH siRNA (Ambion Inc, Austin, TX) or the scrambled siRNA sequence condensed at a N/P ratio of 2.5/1 were incubated with the cells for 6 hours at a final siRNA concentration of 100–200 nM before the addition of fresh culture medium (500  $\mu$ L) and incubating for a total of 48 h. The effect of different treatments on GAPDH expression was quantified based on mRNA and protein levels. Briefly, total RNA was isolated from the cells using the RNeasy Mini Kit (Qiagen Inc, Valencia, CA) and a total of 0.25  $\mu$ g RNA was reverse transcribed using Omniscript reverse transcriptase kit (Qiagen Inc, Valencia, CA) following manufacturer’s protocols. Real-time PCR was performed in a final volume of 20  $\mu$ L containing 2  $\mu$ L of cDNA (corresponding to 10 ng of total RNA for GAPDH and  $\beta$ -actin amplification), 1  $\mu$ L of each primer, and 10  $\mu$ L of the qPCR MasterMix in the 7500 Fast Real-Time PCR system (Life Technologies, Grand Island, NY). The amount of GAPDH protein expressed by cells was measured using the KAlert GAPDH assay (Ambion Inc, Austin, TX) following manufacturer’s specifications. The level of GAPDH protein expression in response to different treatments was normalized to that of untreated control cells.

## Supporting Information

Supporting Information is available from the Wiley Online Library or from the author.

## Acknowledgements

Y.Y.D. and Y.-L.L. contributed equally to this work. This research was partially funded by Susan G. Komen Breast Cancer Foundation.

Received: December 19, 2012

Revised: January 19, 2013

Published online: March 11, 2013

- [1] a) S. M. Elbashir, J. Harborth, W. Lendeckel, A. Yalcin, K. Weber, T. Tuschl, *Nature* **2001**, *411*, 494; b) M. T. McManus, P. A. Sharp, *Nat. Rev. Genet.* **2002**, *3*, 737; c) M. Scherr, M. A. Morgan, M. Eder, *Curr. Med. Chem.* **2003**, *10*, 245; d) L. Timmons, A. Fire, *Nature* **1998**, *395*, 854.
- [2] J. Zhang, Y. O. Wu, L. Xiao, K. Li, L. L. Chen, P. Sirois, *Mol. Biotechnol.* **2007**, *37*, 225.
- [3] A. Hassan, *Recent Pat. Cardiovasc. Drug Discovery* **2006**, *1*, 141.
- [4] a) A. de Fougères, H. P. Vornlocher, J. Maraganore, J. Lieberman, *Nat. Rev. Drug Discovery* **2007**, *6*, 443; b) E. Koutsilieri, A. Rethwilm, C. Scheller, *J. Neural Transm. Suppl.* **2007**, 43.
- [5] a) D. Jere, H. L. Jiang, R. Arote, Y. K. Kim, Y. J. Choi, M. H. Cho, T. Akaïke, C. S. Cho, *Expert Opin. Drug Delivery* **2009**, *6*, 827; b) W. F. Lai, M. C. Lin, *J. Controlled Release* **2009**, *134*, 158; c) P. Midoux, C. Pichon, J. J. Yaouanc, P. A. Jaffres, *Br. J. Pharmacol.* **2009**, *157*, 166; d) T. O. Pangburn, M. A. Petersen, B. Waybrant, M. M. Adil, E. Kokkoli, *J. Biomech. Eng.* **2009**, *131*, 074005.
- [6] a) B. Martin, M. Sainlos, A. Aissaoui, N. Oudrhiri, M. Hauchecorne, J. P. Vigneron, J. M. Lehn, P. Lehn, *Curr. Pharm. Des.* **2005**, *11*, 375; b) D. A. Medvedeva, M. A. Maslov, R. N. Serikov, N. G. Morozova, G. A. Serebrennikova, D. V. Sheglov, A. V. Latushev, V. V. Vlassov, M. A. Zenkova, *J. Med. Chem.* **2009**, *52*, 6558.

- [7] O. Boussif, F. Lezoualc'h, M. A. Zanta, M. D. Mergny, D. Scherman, B. Demeneix, J. P. Behr, *Proc. Natl. Acad. Sci. USA* **1995**, *92*, 7297.
- [8] L. K. Medina-Kauwe, J. Xie, S. Hamm-Alvarez, *Gene Therapy* **2005**, *12*, 1734.
- [9] a) A. S. Hoffman, P. S. Stayton, O. Press, N. Murthy, C. A. Lackey, C. Cheung, F. Black, J. Campbell, N. Fausto, T. R. Kyriakides, P. Bornstein, *Polym. Adv. Technol.* **2002**, *13*, 992; b) P. S. Stayton, M. E. El-Sayed, N. Murthy, V. Bulmus, C. Lackey, C. Cheung, A. S. Hoffman, *Orthod. Craniofac. Res.* **2005**, *8*, 219.
- [10] a) M. E. El-Sayed, A. S. Hoffman, P. S. Stayton, *Expert Opin. Biol. Ther.* **2005**, *5*, 23; b) S. M. Henry, M. E. H. El-Sayed, C. M. Pirie, A. S. Hoffman, P. S. Stayton, *Biomacromolecules* **2006**, *7*, 2407; c) P. S. Stayton, A. S. Hoffman, M. El-Sayed, S. Kulkarni, T. Shimoboji, N. Murthy, V. Bulmus, C. Lackey, *Proc. IEEE* **2005**, *93*, 726.
- [11] P. Schoen, A. Chonn, P. R. Cullis, J. Wilschut, P. Scherrer, *Gene Therapy* **1999**, *6*, 823.
- [12] R. E. Johns, M. E. H. El-Sayed, V. Bulmus, J. Cuschieri, R. Maier, A. S. Hoffman, P. S. Stayton, *J. Biomater. Sci.-Polym. E* **2008**, *19*, 1333.
- [13] Y. L. Lin, G. H. Jiang, L. K. Birrell, M. E. H. El-Sayed, *Biomaterials* **2010**, *31*, 7150.
- [14] C. A. Lackey, O. W. Press, A. S. Hoffman, P. S. Stayton, *Bioconjugate Chem.* **2002**, *13*, 996.
- [15] T. R. Kyriakides, C. Y. Cheung, N. Murthy, P. Bornstein, P. S. Stayton, A. S. Hoffman, *J. Controlled Release* **2002**, *78*, 295.
- [16] M. E. H. El-Sayed, A. S. Hoffman, P. S. Stayton, *J. Controlled Release* **2005**, *104*, 415.
- [17] a) V. Bulmus, M. Woodward, L. Lin, N. Murthy, P. Stayton, A. Hoffman, *J. Controlled Release* **2003**, *93*, 105; b) M. E. H. El-Sayed, A. S. Hoffman, P. S. Stayton, *J. Controlled Release* **2005**, *101*, 47.
- [18] a) M. Kurisawa, M. Yokoyama, T. Okano, *J. Controlled Release* **2000**, *68*, 1; b) N. Murthy, I. Chang, P. Stayton, A. Hoffman, *Macromol. Symp.* **2001**, *172*, 49; c) R. K. Oskuee, A. Dehshahri, W. T. Shier, M. Ramezani, *J. Gene Med.* **2009**, *11*, 921; d) Y. T. Wen, S. R. Pan, X. Luo, X. Zhang, W. Zhang, M. Feng, *Bioconjugate Chem.* **2009**, *20*, 322.
- [19] a) O. Boussif, M. A. Zanta, J. P. Behr, *Gene Ther.* **1996**, *3*, 1074; b) T. Merdan, K. Kunath, H. Petersen, U. Bakowsky, K. H. Voigt, J. Kopecek, T. Kissel, *Bioconjugate Chem.* **2005**, *16*, 785.
- [20] R. M. Schiffelers, A. Ansari, J. Xu, Q. Zhou, Q. Q. Tang, G. Storm, G. Molema, P. Y. Lu, P. V. Scaria, M. C. Woodle, *Nucleic Acids Res.* **2004**, *32*.
- [21] a) S. Boeckle, K. von Gersdorff, S. van der Piepen, C. Culmsee, E. Wagner, M. Ogris, *J. Gene Med.* **2004**, *6*, 1102; b) M. L. Forrest, J. T. Koerber, D. W. Pack, *Bioconjugate Chem.* **2003**, *14*, 934; c) M. Thomas, Q. Ge, J. J. Lu, J. Z. Chen, A. M. Klivanov, *Pharm. Res.* **2005**, *22*, 373.
- [22] a) M. E. Davis, M. E. Brewster, *Nat. Rev. Drug Discovery* **2004**, *3*, 1023; b) E. M. M. Del Valle, *Process Biochem.* **2004**, *39*, 1033; c) K. Uekama, F. Hirayama, T. Irie, *Chem. Rev.* **1998**, *98*, 2045.
- [23] a) D. A. Fulton, J. F. Stoddart, *Org. Lett.* **2000**, *2*, 1113; b) F. Ortega-Caballero, C. O. Mellet, L. Le Gourrierec, N. Guilloteau, C. Di Giorgio, J. Vierling, J. Defaye, J. M. G. Fernandez, *Org. Lett.* **2008**, *10*, 5143; c) S. Srinivasachari, K. M. Fichter, T. M. Reineke, *J. Am. Chem. Soc.* **2008**, *130*, 4618.
- [24] P. van de Wetering, E. E. Moret, N. M. E. Schuurmans-Nieuwenbroek, M. J. van Steenberg, W. E. Hennink, *Bioconjugate Chem.* **1999**, *10*, 589.
- [25] N. J. Zuidam, G. Posthuma, E. T. J. de Vries, D. J. A. Crommelin, W. E. Hennink, G. Storm, *J. Drug Targeting* **2000**, *8*, 51.
- [26] M. Neu, D. Fischer, T. Kissel, *J. Gene Med.* **2005**, *7*, 992.
- [27] a) K. S. Pafiti, N. P. Mastroyiannopoulos, L. A. Phylactou, C. S. Patrickios, *Biomacromolecules* **2011**, *12*, 1468; b) F. J. Xu, Z. X. Zhang, Y. Ping, J. Li, E. T. Kang, K. G. Neoh, *Biomacromolecules* **2009**, *10*, 285; c) F. Y. Dai, P. Sun, Y. J. Liu, W. G. Liu, *Biomaterials* **2010**, *31*, 559.
- [28] C. V. Synatschke, A. Schallon, V. Jerome, R. Freitag, A. H. E. Muller, *Biomacromolecules* **2011**, *12*, 4247.
- [29] E. R. Gillies, J. M. J. Frechet, *J. Am. Chem. Soc.* **2002**, *124*, 14137.
- [30] B. Newland, H. Y. Tai, Y. Zheng, D. Velasco, A. Di Luca, S. M. Howdle, C. Alexander, W. X. Wang, A. Pandit, *Chem. Commun.* **2010**, *46*, 4698.
- [31] a) P. vandeWetering, J. Y. Cherng, H. Talsma, W. E. Hennink, *J. Controlled Release* **1997**, *49*, 59; b) J. M. Layman, S. M. Ramirez, M. D. Green, T. E. Long, *Biomacromolecules* **2009**, *10*, 1244; c) T. K. Georgiou, M. Vamvakaki, C. S. Patrickios, E. N. Yamasaki, L. A. Phylactou, *Biomacromolecules* **2004**, *5*, 2221.
- [32] a) J. S. Wang, K. Matyjaszewski, *J. Am. Chem. Soc.* **1995**, *117*, 5614; b) M. Kato, M. Kamigaito, M. Sawamoto, T. Higashimura, *Macromolecules* **1995**, *28*, 1721.
- [33] a) F. Ganachaud, M. J. Monteiro, R. G. Gilbert, M. A. Dourges, S. H. Thang, E. Rizzardo, *Macromolecules* **2000**, *33*, 6738; b) J. Chiefari, Y. K. Chong, F. Ercole, J. Krstina, J. Jeffery, T. P. T. Le, R. T. A. Mayadunne, G. F. Meijs, C. L. Moad, G. Moad, E. Rizzardo, S. H. Thang, *Macromolecules* **1998**, *31*, 5559.
- [34] a) H. Liu, X. Z. Jiang, J. Fan, G. H. Wang, S. Y. Liu, *Macromolecules* **2007**, *40*, 9074; b) F. J. Xu, H. Z. Li, J. Li, Z. X. Zhang, E. T. Kang, K. G. Neoh, *Biomaterials* **2008**, *29*, 3023; c) A. W. York, S. E. Kirkland, C. L. McCormick, *Adv. Drug Delivery Rev.* **2008**, *60*, 1018.
- [35] Y. A. Ping, C. D. Liu, G. P. Tang, J. S. Li, J. Li, W. T. Yang, F. J. Xu, *Adv. Funct. Mater.* **2010**, *20*, 3106.
- [36] T. K. Georgiou, M. Vamvakaki, L. A. Phylactou, C. S. Patrickios, *Biomacromolecules* **2005**, *6*, 2990.
- [37] a) M. R. Park, K. O. Han, I. K. Han, M. H. Cho, J. W. Nah, Y. J. Choi, C. S. Cho, *J. Controlled Release* **2005**, *105*, 367; b) R. Qi, Y. Gao, Y. Tang, R. R. He, T. L. Liu, Y. He, S. Sun, B. Y. Li, Y. B. Li, G. Liu, *AAPS J.* **2009**, *11*, 395.
- [38] F. Yuan, M. Dellian, D. Fukumura, M. Leunig, D. A. Berk, V. P. Torchilin, R. K. Jain, *Cancer Res.* **1995**, *55*, 3752.
- [39] M. Neu, D. Fischer, T. Kissel, *J. Gene Med.* **2005**, *7*, 992.
- [40] a) S. M. Simon, *Drug Discovery Today* **1999**, *4*, 32; b) S. L. Rybak, F. Lanni, R. F. Murphy, *Biophys. J.* **1997**, *73*, 674; c) C. C. Cain, D. M. Sipe, R. F. Murphy, *Proc. Natl. Acad. Sci. USA* **1989**, *86*, 544.
- [41] a) O. A. Weisz, *Traffic* **2003**, *4*, 57; b) M. Duvvuri, S. Konkar, K. H. Hong, B. S. J. Blagg, J. P. Krise, *ACS Chem. Biol.* **2006**, *1*, 309; c) S. Simon, D. Roy, M. Schindler, *Proc. Natl. Acad. Sci. USA* **1994**, *91*, 1128.
- [42] B. Zhang, S. Mallapragada, *Acta Biomater.* **2011**, *7*, 1580.
- [43] A. Imai, B. D. Zeitlin, F. Visioli, Z. H. Dong, Z. C. Zhang, S. Krishnamurthy, E. Light, F. Worden, S. M. Wang, J. E. Nor, *Cancer Res.* **2012**, *72*, 716.